Biochemical and Biophysical Research Communications 446 (2014) 775–781

Contents lists available at ScienceDirect

Biochemical and Biophysical Research Communications

journal homepage: www.elsevier.com/locate/ybbrc

In vivo consequences of cholesterol-24S-hydroxylase (CYP46A1) inhibition by voriconazole on cholesterol homeostasis and function in the rat retina

Cynthia Fourgeux [a,b,c,*], Lucy Martine [a,b,c], Niyazi Acar [a,b,c], Alain M. Bron [a,b,c,d], Catherine P. Creuzot-Garcher [a,b,c,d], Lionel Bretillon [a,b,c]

[a] INRA, UMR1324 Centre des Sciences du Goût et de l'Alimentation, Eye and Nutrition Research Group, F-21000 Dijon, France
[b] CNRS, UMR6265 Centre des Sciences du Goût et de l'Alimentation, F-21000 Dijon, France
[c] Université de Bourgogne, Centre des Sciences du Goût et de l'Alimentation, F-21000 Dijon, France
[d] University Hospital, Department of Ophthalmology, F-21000 Dijon, France

ARTICLE INFO

Article history:
Available online 1 February 2014

Keywords:
Retinal ganglion cell
Glia
Cholesterol homeostasis
CYP46A1
Voriconazole

ABSTRACT

Cholesterol 24S-hydroxylase (CYP46A1) converts cholesterol into 24S-hydroxycholesterol in neurons and participates in cholesterol homeostasis in the central nervous system, including the retina. We aimed to evaluate the consequences of CYP46A1 inhibition by voriconazole on cholesterol homeostasis and function in the retina. Rats received daily intraperitoneal injections of voriconazole (60 mg/kg), minocycline (22 mg/kg), voriconazole *plus* minocycline, or vehicle during five consecutive days. The rats were submitted to electroretinography to monitor retinal functionality. Cholesterol and 24S-hydroxycholesterol were measured in plasma, brain and retina by gas chromatography-mass spectrometry. The expression of CYP46A1, and GFAP as a marker for glial activation was analyzed in the retina and brain. Cytokines and chemokines were measured in plasma, vitreous, retina and brain. Voriconazole significantly impaired the functioning of the retina as exemplified by the reduced amplitude and increased latency of the b-wave of the electroretinogram, and altered oscillary potentials. Voriconazole decreased 24S-hydroxycholesterol levels in the retina. Unexpectedly, CYP46A1 and GFAP expression was increased in the retina of voriconazole-treated rats. ICAM-1 and MCP-1 showed significant increases in the retina and vitreous body. Minocycline did not reverse the effects of voriconazole. Our data highlighted the cross talk between retinal ganglion cells and glial cells in the retina, suggesting that reduced 24S-hydroxycholesterol concentration in the retina may be detected by glial cells, which were consequently activated.

1. Introduction

Free cholesterol accounts for 85% of total cholesterol in the neurosensory retina, the remaining consists of cholesteryl esters [1]. Dysregulations of cholesterol homeostasis leading to cholesterol deficiency or accumulation have detrimental consequences on the retina and are associated with neurodegeneration [2]. As an example, the Smith–Lemli–Opitz syndrome that is due to 7-dehydrocholesterol reductase deficiency [3] causes the inability of the cells to synthesize cholesterol, results to the accumulation of 7-dehydrocholesterol in brain [4], retinal neurons [5] and is associated with neurodegeneration. Cholesterol accumulation in Niemann-Pick type C syndrome gives a similar feature of loss of neurons in the brain [6] and retina [7].

Cholesterol 24S-hydroxylase (CYP46A1), cholesterol-27-hydroxylase (CYP27A1) and CYP11A1 are cholesterol-metabolizing enzymes that are involved in cholesterol homeostasis, and are expressed in the retina [8]. Cholesterol 24S-hydroxylase (CYP46A1) converts cholesterol into 24S-hydroxycholesterol (24SOH) in neurons of the central nervous system [9]. CYP46A1 expression and 24SOH are specific to neurons of the CNS [10], including inner neurons of the retina and retinal ganglion cells (RGC) [10,11]. The exact role of CYP46A1 in the retina remains partly unknown. Alike brain neurons [9] the formation of 24SOH may represent a pathway for retinal neurons to maintain the balance of cholesterol. Interestingly, in an experimental rat model of glaucoma, we found steady-states levels of CYP46A1 and 24SOH in the retina, despite the expected loss of retinal neurons and as a consequence, the expected decrease in CYP46A1 and 24SOH levels [12].

* Corresponding author at: CSGA, Centre INRA, 17 rue Sully, F-21000 Dijon, France. Fax: +33 380693223.
E-mail address: cynthia.fourgeux@dijon.inra.fr (C. Fourgeux).

http://dx.doi.org/10.1016/j.bbrc.2014.01.118
0006-291X/

Voriconazole is an antifungal agent that inhibits CYP46A1 with high affinity in mice brain [13]. In vitro, voriconazole potentiated the activation of monocytes triggered by fungal infection, especially by up-regulating the expression of immunomodulatory genes, including TNF-α [14]. The safety of intravitreous injection of voriconazole on the function of the retina has been established in rats [15] and rabbits [16]. On the contrary, when injected intravenously, voriconazole transiently impaired bipolar cell function in monkeys [17]. The reason for the discrepant data in the simian species compared to rodents and rabbits may be linked to the systemic effect of voriconazole on monocyte activation [14] that may infiltrate the retina when voriconazole was used intravenously. On the contrary, such inflammatory process would not occur when used intravitreally. Retinal impairment may alternatively be associated to the inhibition of CYP46A1 in retinal cells that specifically express CYP46A1. Until now the role of CYP46A1 in the electrophysiological response of the retinal cells remains unknown.

To better understand the role of CYP46A1 in the retina, we took advantage of voriconazole as an inhibitor of CYP46A1 activity to evaluate its potential to modulate cholesterol homeostasis and function in the retina. Meanwhile, minocycline was used in parallel and in addition to voriconazole to inhibit monocyte activation, and therefore delineate the specific effects of voriconazole in this pathway.

2. Materials and methods

All animals were handled according to the regulations of the Institutional Animal Care Committee (University of Burgundy, Dijon, France), and all procedures adhered to the tenets of the statements of the Association for Research in Vision and Ophthalmology for the use of Animals in Ophthalmic and Vision Research.

2.1. Voriconazole and minocycline administration

Fifty male Wistar rats (7–8 weeks of age, Elevage Janvier, Le Genest Saint Isle, France) were maintained under pathogen-free conditions of temperature (22 ± 1 °C), hygrometry (55–60%) and light (50 lux, from 07:00 am to 07:00 pm). The rats received intraperitoneal injections of either voriconazole (Vor) (60 mg/kg in PBS 1x, once a day, $n = 15$) (Pfizer, Groton, USA), minocycline (Mino) (22 mg/kg in PBS 1x, once a day, $n = 10$) (Sigma–Aldrich, Saint Quentin Fallavier, France), voriconazole *plus* minocycline (Vor + Mino) (60 and 22 mg/kg respectively in PBS 1x, $n = 10$), or vehicle (0.2 mL PBS 1x, once a day, $n = 15$) during five consecutive days.

2.2. Electroretinography (ERG)

Before ERG recordings, the rats ($n = 10$ per group) were dark-adapted for at least 12 h. Further procedures were carried out under dim red light ($\lambda = 650$ nm) and at a constant temperature of 25 °C. Animal anaesthesia, pupil dilatation, corneal hydratation and ERG measurements were carried out as described [18] with the following modifications. The band-pass filter width was 1–300 Hz for the recording procedure of scotopic single-flash responses. Stimuli of the scotopic single-flash were recorded with ten increasing intensities from 0.0003 to 10 cd.s/m^2. These responses were averaged with an inter-stimulus interval of 5 s (from 1 to 10 cd.s/m^2) or 17 s (up to 0.3 cd.s/m^2). The band-pass filter width was 0.2–30 Hz for the recording procedure of scotopic threshold responses (STR). Stimuli of the STR were recorded with three increasing intensities: −4.60 log, −4.32 log and −4.02 log cd.s/m^2, with an inter-stimulus interval of 2 s. For the oscillatory potentials (OPs) recording, the band-pass filter width was 200–500 Hz. One single stimulus was applied at 0.06 Hz. The inter-stimuli interval was about 17 s. After amplification, the signal was digitized and processed.

The a- and b-waves amplitudes and latencies of the scotopic and photopic responses were analyzed as previously described [19]. OPs were recorded as previously published [20] and analyzed on the basis of means of amplitude and time-latency measurements of each of the four peaks [21].

2.3. Sample processing

After ERG recordings, rats were euthanized. Eyeballs were removed. Blood (5 mL in EDTA) was taken by aortic puncture and plasma was prepared by 15-min centrifugation at 3000 rpm at 4 °C. Vitreous of both eyes was collected and pooled for each animal ($n = 10$ per group). Retinas were dissected from the underlying choroid and sclera. For each animal, one retina was stored at −20 °C in 2 mL of 1 M KOH for 24SOH and cholesterol quantification ($n = 10$ per group) (see paragraph 2.4). The other retina was snap-frozen at −80 °C until whole protein extraction ($n = 10$ per group). The retinal lysates were further divided for cytokines/chemokines quantification (see paragraph 2.5) and Western blotting (see paragraph 2.6). Brains were dissected sagitally and divided in two parts. One half-brain was stored in 5 mL of chloroform/methanol (2:1, v/v) for 24SOH and cholesterol quantification ($n = 10$ per group) and 10 mg cortex was used for cytokines/chemokines quantification and Western blotting ($n = 10$ per group).

2.4. Quantification of cholesterol and 24-hydroxycholesterol in the retina, brain and plasma

Total lipids were extracted from the brains as described [22]. Plasma and retina were processed as previously published [12]. Cholesterol and 24SOH were quantified from one tenth of the lipid extract in one single retina ($n = 10$ per group), plasma ($n = 10 \times 1$ mL per group) and a half-brain ($n = 10$ per group) using authentic internal standards: 5α-cholestane (5 μg in plasma and retina, 10 μg in the brain) for cholesterol quantification, and deuterated racemic [23,23,24-$^2H_3$]-24-hydroxycholesterol (generous gift from Pr Björkhem, Karolinska Institutet, Stockholm, Sweden) for 24SOH quantification (100 ng in plasma and retina, 150 ng in the brain).

2.5. Quantification of cytokines, chemokines and growth factors in plasma, vitreous, retina and cortex homogenates

IL6, MCP-1, VEGF, IL1β, ICAM-1 and TNFα were quantified simultaneously in plasma, vitreous, retinal and brain homogenates with Procarta® Cytokine Assay kit (Affymetrix, Santa Clara, USA). Cytokines and chemokines were measured by Luminex® with the BioPlex® software (BioRad Laboratories, Hercules, USA) and expressed as picograms per milligram of total proteins analyzed using the bicinchoninic acid assay (Pierce, Rockford, USA).

2.6. CYP46A1 and GFAP expression levels in the retina and cortex

Technical procedures to complete Western-blotting (from 25 μg of total proteins) and revelation protocols were reproduced as previously described [12] using the following primary antibodies: polyclonal rabbit anti-GFAP (clone N-18, 1:2000 dilution) and monoclonal mouse anti-CYP46A1 antibody (clone 1F11, 1:1000) (Santa Cruz Biotechnology Inc., Santa Cruz, USA). The secondary antibodies were goat anti-rabbit and goat anti-mouse HRP-linked antibodies, respectively (1:4000, Dako A/S, Denmark). The signal was quantified by comparison with monoclonal mouse anti-β-tubulin (dilution 1:4000, Zymed Laboratories, South San Francisco,

USA) as a gel-loading control and revealed with the same anti-mouse secondary antibody as described above.

2.7. Statistical analyses

A nonparametric Kruskal–Wallis test was used to compare protein expression levels, 24SOH/cholesterol amounts, cytokines and chemokines between groups. The relationship between each outcome (GFAP, CYP46A1, 24SOH, cytokines and chemokines) and each of the explanatory variables (sample and group) was modeled as a generalized estimating equation (GEE), to account for the correlated nature of the data. A robust variance estimator was used. The explanatory variables – sample (plasma, vitreous, retina and brain) and group (no intervention or intervention) – were binary coded. Dunn's comparison test was used. All analyses were conducted using STATA version 12.0 (STATACORP, College Station, USA). The level of statistical significance was set at $p < 0.05$ and the tests were two-tailed.

3. Results

3.1. Impairment of retinal functionality

Voriconazole injected alone or with minocycline significantly impaired the function of the inner retina as exemplified by the reduced b-wave amplitude (Fig. 1). ERG b-wave latency was unaffected by voriconazole. Minocycline alone had no effect on the ERG. The a-wave amplitude was unaffected by any treatment compared to control, whereas a-wave latency was slightly but not significantly increased after Vor and Vor + Mino injections (data not shown). OPs were altered by Vor, and Vor + Mino, especially when considering P2 and P3 peaks and the sum of the four individual OPs ($p < 0.0001$, Fig. 2a). Time latencies of the pSTR and nSTR were unaffected by the treatments (data not shown). At higher light intensities, pSTR and nSTR were significantly decreased in Vor + -Mino group ($p < 0.0002$) (Fig. 2b and c). At the lower intensity, pSTR were significantly decreased in Vor group only ($p < 0.05$). On the contrary to the vehicle and minocycline groups, pSTR amplitudes did not increase as a function of light stimulus intensity in animals treated with Vor and Vor + Mino, suggesting specific effects of voriconazole on retinal function.

3.2. Dysregulation of cholesterol homeostasis

24SOH levels decreased by 37% ($p < 0.05$) and 25% (not significant) in the retina of Vor and Vor + Mino groups, respectively, compared to the control group (Fig. 3). In the brain, 24SOH levels were unaffected by Vor but were decreased by 43% in the Vor + Mino group ($p < 0.001$, Fig. 3). Plasma 24SOH concentrations were significantly decreased by 45% ($p < 0.005$) in the Vor + Mino groups, 18% and 16% in the Vor and Mino groups respectively (not significant, Fig. 3). Moreover, minor changes in cholesterol levels were found in the retina: −12% in Vor + Mino group ($p < 0.05$) compared to Vor group in which levels reached +18% of the value in the group injected with vehicle (not significant).

3.3. Up-regulation of CYP46A1 and GFAP expression in the retina and cortex

CYP46A1 expression was increased in the retina and cortex of the Vor group (x1.4 and x1.2, respectively, compared to control) and in the Vor + Mino group (x1.7 and x1.3, respectively, compared to control) but the differences were not significant (Fig. 4). Meanwhile, GFAP expression was raised by a factor of 2.7 and 4.3 in the retina ($p < 0.05$) and 1.8 and 1.6 in the cortex (not significant), after Vor and Vor + Mino treatments respectively, compared to control (Fig. 4). Interestingly, the levels of CYP46A1 expression in the retina and the cortex were positively associated ($R^2 = 0.241$; $p = 0.0013$). The same positive association was observed between CYP46A1 and GFAP expression in the retina ($R^2 = 0.298$, $p = 0.0003$).

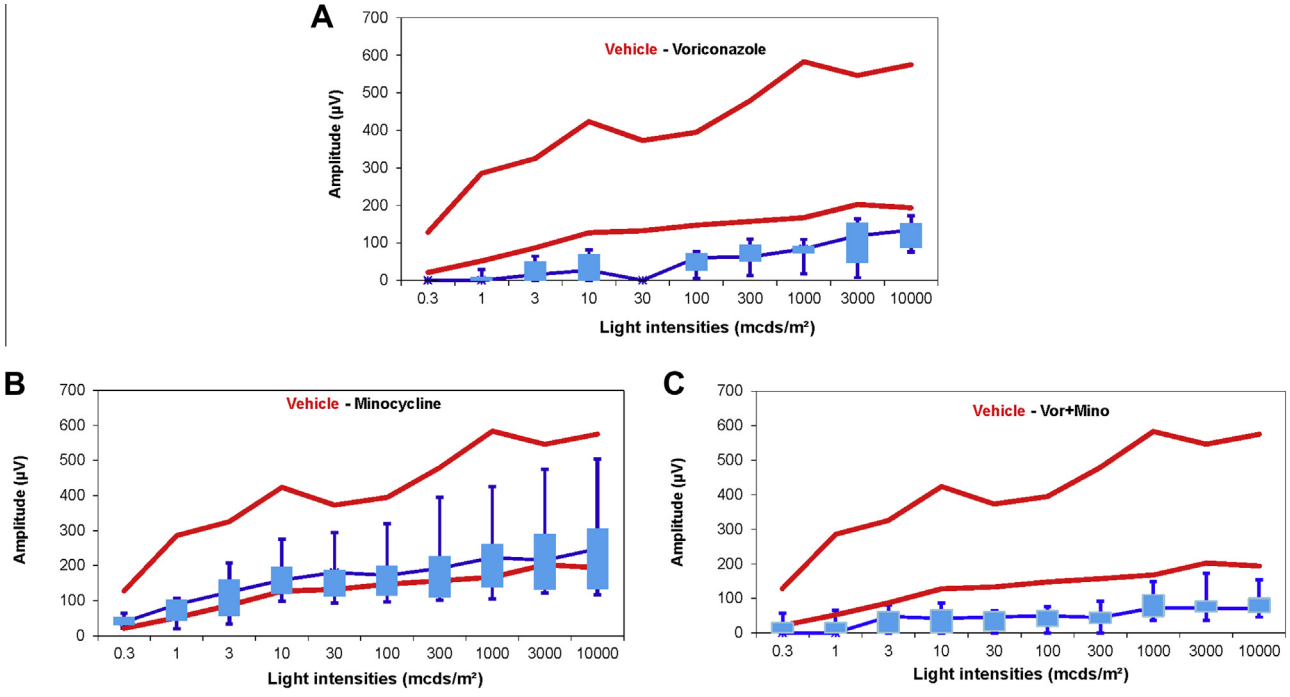

Fig. 1. Scotopic b-wave amplitude of the ERG after 5 days of intraperitoneal injections of voriconazole ($n = 15$) (a), minocycline ($n = 10$) (b) and voriconazole + minocycline ($n = 10$) (c) (in blue) compared to vehicle ($n = 15$). Normal range given by the 5% and 95% quantile of the rats treated with vehicle is shown by red lines. Data are plotted as a function of the flash intensity.

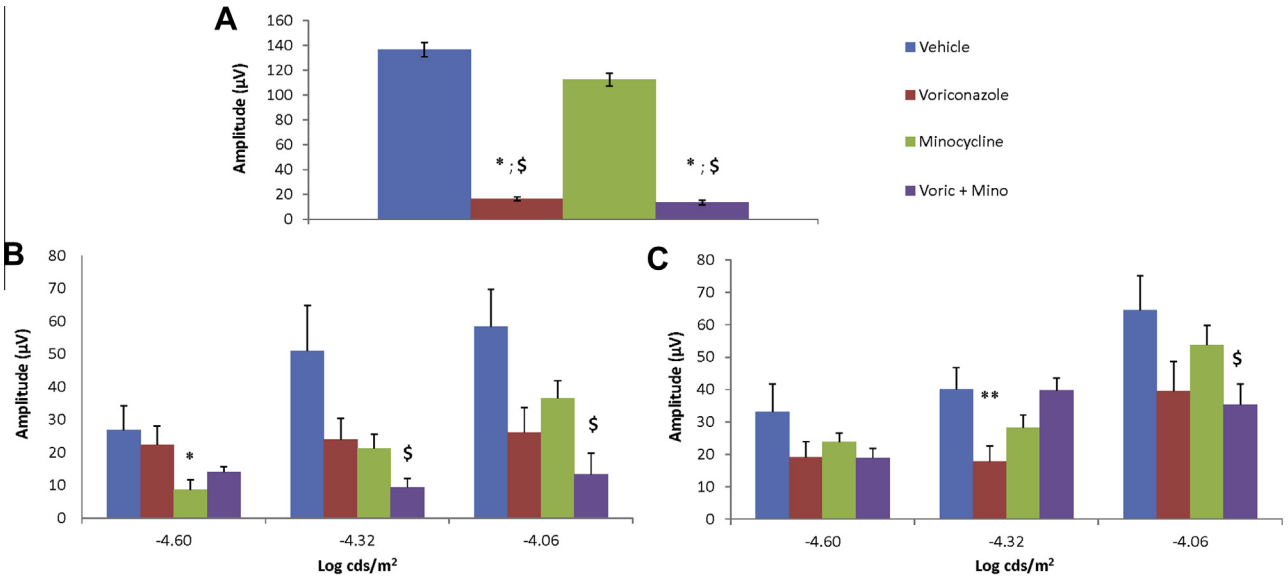

Fig. 2. (a) Sum of mean amplitudes of the four oscillatory potentials recorded during ERG processing and displayed as histogram. *: significantly different from vehicle ($n = 15$) at $p < 0.0001$. $: significantly different from minocycline ($n = 10$) at $p < 0.0001$. Means of pSTR (b) and nSTR (c) measured in each eye at the time of ERG recording. *, **, $: significantly different at $p < 0.02$; $p < 0.002$ and $p < 0.0002$, respectively in each group compared to vehicle.

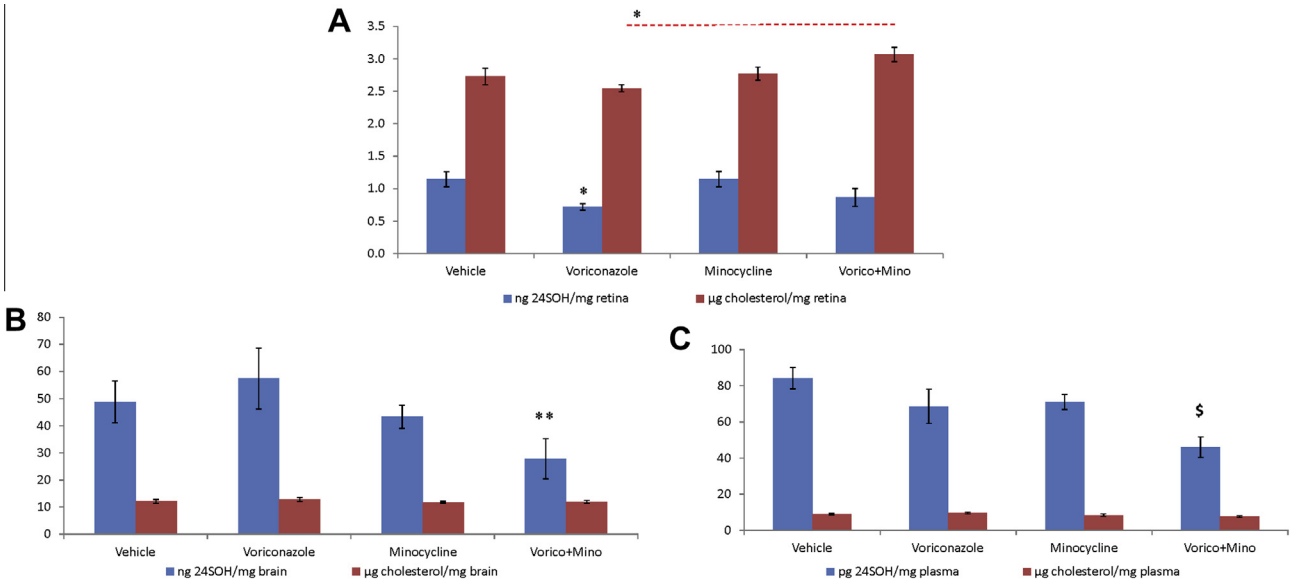

Fig. 3. Changes of 24SOH and cholesterol levels in the retina (a), brain (b) and plasma (c) after 5 days of intraperitoneal injections with voriconazole (Vor), minocycline (Mino) or voriconazole + minocycline (Vor + Mino) ($n = 10$ per group). Data are expressed as means ± SEM. (a) *: significantly different from 24SOH in the retina of Vor group compared to vehicle at $p < 0.05$; * with reds dots: significantly different from cholesterol in the retina of Vor + Mino group compared to Vor group. (b) **: significantly different from 24SOH in the brain of Vor + Mino groups at $p < 0.001$. (c) $: significantly different from 24SOH in the plasma of Vor + Mino groups at $p < 0.005$.

Minocycline did not reverse the effects of voriconazole. CYP46A1 and the retina and cortex GFAP expression remained unaffected by minocycline injection compared to vehicle.

3.4. Measurement of cytokines, chemokines and growth factors in plasma, vitreous body, retina and cortex homogenates

The results of cytokines and chemokines measurements are shown in the table. Voriconazole significantly increased plasma MCP-1 concentration by 1.5-fold, and decreased VEGF levels by 65% in the vitreous body. Minocycline decreased by half TNFα in the cortex. The most tremendous effects were found after Vor + Mino treatment. MCP-1 and ICAM-1 levels were significantly increased 2.3-fold in the retina and 12-fold in the vitreous compared to vehicle. IL6 was also significantly increased in the vitreous of Vor + Mino groups (x12.5) compared to vehicle (Table 1).

4. Discussion

Among azoles that bind CYP46A1 [23], voriconazole inhibits CYP46A1 and cholesterol biosynthesis in mice brain [13]. Until now the question about similar effects of this molecule in the retina remained unknown. Similar to the brain, CYP46A1 is specifically expressed in neurons of the neural retina [11], on the contrary to other CYP450 enzymes, such as CYP27A1 and CYP11A1 which are expressed in the retina but are not specific to neurons

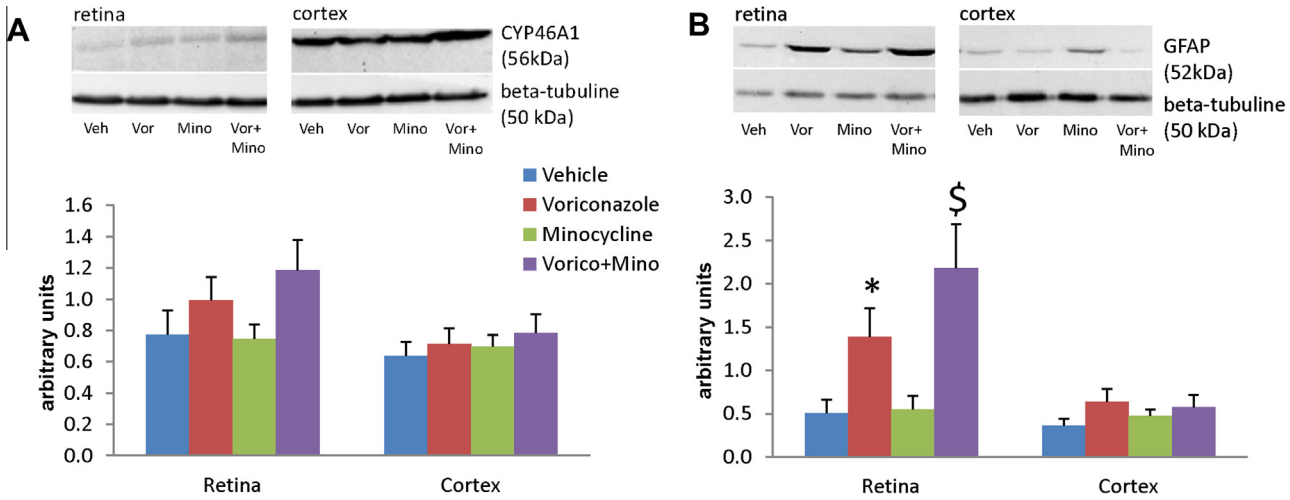

Fig. 4. CYP46A1 (a) and GFAP (b) expression in experimental retinas and cortex (n = 10 per group each). Values are expressed in arbitrary units as means ± SEM. Blots issued from the BioRad molecular imager are shown in each graph. *, $: significantly different from the value in the retina of Vor and Vor + Mino groups compared to vehicle at $p < 0.05$ or $p < 0.002$, respectively.

Table 1
Mean X-fold values related to vehicle of each cytokines or chemokines expressed as pg/mg of total proteins in the corresponding tissues or body fluids.

		MCP-1	ICAM-1	IL1b	IL6	VEGF	TNFa
Retina							
	Vehicle	1.00 ± 0.09	1.00 ± 0.13	1.00 ± 0.03	1.00 ± 0.13	1.00 ± 0.04	1.00 ± 0.07
	Voriconazole	1.17 ± 0,13	1.18 ± 0.21	1.13 ± 0.06	1.31 ± 0.17	0.91 ± 0.09	0.89 ± 0.10
	Minocycline	0.95 ± 0.07	0.86 ± 0.12	0.89 ± 0.06	0.94 ± 0.17	0.89 ± 0.05	0.90 ± 0.07
	Vori + Mino	2.32 ± 0.42$^{\$,£}$	1.68 ± 0.21**	1.11 ± 0.07**	1.29 ± 0.28	0.91 ± 0.10	1.11 ± 0.10
Cortex							
	Vehicle	1.00 ± 0.05	1.00 ± 0.11	1.00 ± 0.05	1.00 ± 0.14	1.00 ± 0.06	1.00 ± 0.11
	Voriconazole	0.96 ± 0.13	0.92 ± 0.11	0.96 ± 0.12	0.78 ± 0.16	1.02 ± 0.09	0.74 ± 0.13
	Minocycline	0.84 ± 0.09	0.89 ± 0.13	0.90 ± 0.08	0.75 ± 0.15	0.89 ± 0.06	0.44 ± 0.06*
	Vori + Mino	0.90 ± 0.07	0.99 ± 0.20	0.87 ± 0.08	0.84 ± 0.09	0.82 ± 0.05	0.98 ± 0.19
Vitreous							
	Vehicle	1.00 ± 0.18	1.00 ± 0.12	1.00 ± 0.19	1.00 ± 0.39	1.00 ± 0.18	1.00 ± 0.17
	Voriconazole	3.18 ± 1.74	1.79 ± 0.52	1.35 ± 0.67	1.99 ± 1.09	0.35 ± 0.11 $^{**,\mu}$	1.05 ± 0.21
	Minocycline	3.09 ± 0.70	1.82 ± 0.35	1.30 ± 0.33	2.67 ± 1.13	1.24 ± 0.27	1.17 ± 0.17
	Vori + Mino	12.45 ± 4.28$^{\$,£}$	2.67 ± 0.63 *	1.60 ± 0.51	12.50 ± 3.64 $^{**,\&}$	0.34 ± 0.06 $^{**,\mu}$	0.89 ± 0.19
Plasma							
	Vehicle	1.00 ± 0.08	1.00 ± 0.06	1.00 ± 0.09	1.00 ± 0.07	1.00 ± 0.36	1.00 ± 0.48
	Voriconazole	1.51 ± 0.16*	1.19 ± 0.17	1.33 ± 0.37	0.74 ± 0.06	3.88 ± 1.45	8.99 ± 3.96
	Minocycline	1.42 ± 0.15	0.78 ± 0.06	0.71 ± 0.09	0.99 ± 0.14	1.70 ± 0.86	0.80 ± 0.41
	Vori + Mino	1.25 ± 0.08	1.01 ± 0.11	0.84 ± 0.10	1.01 ± 0.08	1.82 ± 0.86	1.10 ± 0.49

Mean X-fold values related to vehicle of each cytokines or chemokines expressed as pg/mg of total proteins in the corresponding tissues or body fluids.
$^{\$,£}$ Significantly different from the value in the corresponding samples at $p < 0.05$ compared to vehicle.
* Significantly different from the value in the corresponding samples at $p < 0.05$ compared to vehicle.
** Significantly different from the value in the vitreous at $p < 0.02$ compared to vehicle and to voriconazole group (&) or minocycline group (μ).

[8]. Intravitreal injection of voriconazole is recommended in the treatment of fungal endophthalmitis and its inocuity was demonstrated in rats [15] and rabbits [16]. When injected intravenously, voriconazole transiently impaired bipolar cell function [17]. In our model, intraperitoneal voriconazole efficiently impaired the functioning of the inner retina as demonstrated by the tremendous reduction of the ERG b-wave amplitude and alteration of the OPs. Similar to Kinoshita's [17], photoreceptors were unaffected since a-wave amplitude was unchanged. The STR recordings showed significant alterations whereas nSTR were not or at least not significantly affected. Cuenca et al. [24] pointed out the relevance to interpret pSTR rather than nSTR. Vidal-Sanz has been a pioneer in the evaluation of STRs in its models of acute RGC loss which surmised the use of STRs to assess RGC dysfunction [25]. Our data clearly highlighted that the inhibition of CYP46A1 in RGC which specifically expressed CYP46A1 [10,11] impaired RGC function. Therefore cholesterol homeostasis seems needed for proper RGC function.

The level of CYP46A1 expression in the retina was slightly but not significantly increased in Vor and Vor + Mino groups, when compared to the control group. Meanwhile GFAP protein was significantly up-regulated in Vor and Vor + Mino groups, suggesting that the inhibition of CYP46A1 activity triggered glial reactivity. Consistently, we found a positive association between CYP46A1 and GFAP expression levels in the retina. This is in accordance with our previous work in a rat model of glaucoma since we suggested that retinal glial cells were able to express CYP46A1 in order to counterbalance the suffering or loss of RGC [12]. Again, as we previously reported [12], the reduction of 24SOH in the retina was associated with up-regulation of GFAP and CYP46A1. Our

interpretation is that retinal glial cells could sense the changes of 24SOH concentration in the retina by over-expression of CYP46A1. The Vor-induced decrease in 24SOH levels observed in the retina but not in the brain can be linked to the greater permeability of the blood-retinal barrier to voriconazole compared to the blood–brain barrier, as previously observed by our group with dietary fatty acids [26]. Of note, 24SOH diminished in the brain and plasma of rats injected with Vor + Mino. Accounting the almost exclusive cerebral origin of 24SOH, the reduction in plasma 24SOH levels is consistent with similar reduced levels in the brain.

In combination with minocycline voriconazole had marked effects on the inflammatory status of the retina and vitreous body, as exemplified by increased levels of MCP-1 and GFAP signal in the retina. Müller cells are major producers of MCP-1 in the retina that is able to attract microglial cells and monocytes/macrophages upon retinal stress [27,28]. Our data revealed that the inhibition of microglia by minocycline exacerbated the effects of voriconazole on the activation of glia and up-regulation of CYP46A1 in the retina. The protective effects of microglial inhibition by minocycline was reported in glaucoma, diabetic retinopathy or even photoreceptor loss [29–31]. Inhibition of microglial activation might be a therapeutic strategy to slow RGC loss [32]. Accounting the enhanced macroglial reactivity and inflammatory markers in the retina and vitreous after voriconazole and minocycline treatment, the neuroprotective effect of microglial inhibition by minocycline may be hampered by CYP46A1 inhibition. Further ongoing experiments will define the consequences of inhibiting CYP46A1 activity in the course of RGC loss in glaucoma models.

Our study supports the role of CYP46A1 in the maintenance of RGC function. Dysregulation of cholesterol homeostasis by voriconazole impaired inner retinal neurons and RGC response. Our data also highlighted the cross talk between RGC and glial cells in the retina by suggesting that reduced 24SOH concentration in the retina may be detected by glial cells which were consequently activated. Our work also showed a close interaction between cholesterol homeostasis in the retina and microglia.

Acknowledgments

We acknowledge the European Regional Development Fund (FEDER) and the Regional Counil of Burgundy for funding part of this work. Voriconazole was obtained from Pfizer laboratories. We also acknowledge the fruitful collaboration with Laboratoires Fournier/Solvay/Abbott (Daix, France) for multiplex analysis of cytokines (Luc Lebreton, Jocelyne Annat, Séverine Delaporte). We are grateful to Bruno Pasquis and Laurence Decoq from Equipe Animalerie Expérimentale du CSGA to take care on animals.

No author has any financial and commercial relationship related to this work to disclose.

References

[1] L. Bretillon, G. Thuret, S. Gregoire, N. Acar, C. Joffre, A.M. Bron, P. Gain, C.P. Creuzot-Garcher, Lipid and fatty acid profile of the retina, retinal pigment epithelium/choroid, and the lacrimal gland, and associations with adipose tissue fatty acids in human subjects, Exp. Eye Res. 87 (2008) 521–528.

[2] S.J. Fliesler, L. Bretillon, The ins and outs of cholesterol in the vertebrate retina, J. Lipid Res. 51 (2010) 3399–3413.

[3] G.S. Tint, M. Irons, E.R. Elias, A.K. Batta, R. Frieden, T.S. Chen, G. Salen, Defective cholesterol biosynthesis associated with the Smith–Lemli–Opitz syndrome, N. Engl. J. Med. 330 (1994) 107–113.

[4] L. Xu, K. Mirnics, A.B. Bowman, W. Liu, J. Da, N.A. Porter, Z. Korade, DHCEO accumulation is a critical mediator of pathophysiology in a Smith–Lemli–Opitz syndrome model, Neurobiol. Dis. 45 (2012) 923–929.

[5] F.L. Kretzer, H.M. Hittner, R.S. Mehta, Ocular manifestations of the Smith–Lemli–Opitz syndrome, Arch. Ophthalmol. 99 (1981) 2000–2006.

[6] S.E. Phillips, E.A. Woodruff 3rd, P. Liang, M. Patten, K. Broadie, Neuronal loss of *Drosophila* NPC1a causes cholesterol aggregation and age-progressive neurodegeneration, J. Neurosci. 28 (2008) 6569–6582.

[7] T. Claudepierre, M. Paques, M. Simonutti, I. Buard, J. Sahel, R.A. Maue, S. Picaud, F.W. Pfrieger, Lack of Niemann-Pick type C1 induces age-related degeneration in the mouse retina, Mol. Cell. Neurosci. 43 (2010) 164–176.

[8] N. Mast, R. Reem, I. Bederman, S. Huang, P.L. DiPatre, I. Bjorkhem, I.A. Pikuleva, Cholestenoic acid is an important elimination product of cholesterol in the retina: comparison of retinal cholesterol metabolism with that in the brain, Invest. Ophthalmol. Vis. Sci. 52 (2011) 594–603.

[9] I. Bjorkhem, D. Lutjohann, O. Breuer, A. Sakinis, A. Wennmalm, Importance of a novel oxidative mechanism for elimination of brain cholesterol. Turnover of cholesterol and 24(S)-hydroxycholesterol in rat brain as measured with 18O2 techniques in vivo and in vitro, J. Biol. Chem. 272 (1997) 30178–30184.

[10] D.M. Ramirez, S. Andersson, D.W. Russell, Neuronal expression and subcellular localization of cholesterol 24-hydroxylase in the mouse brain, J. Comp. Neurol. 507 (2008) 1676–1693.

[11] L. Bretillon, U. Diczfalusy, I. Bjorkhem, M.A. Maire, L. Martine, C. Joffre, N. Acar, A. Bron, C. Creuzot-Garcher, Cholesterol-24S-hydroxylase (CYP46A1) is specifically expressed in neurons of the neural retina, Curr. Eye Res. 32 (2007) 361–366.

[12] C. Fourgeux, L. Martine, B. Pasquis, M.A. Maire, N. Acar, C. Creuzot-Garcher, A. Bron, L. Bretillon, Steady-state levels of retinal 24S-hydroxycholesterol are maintained by glial cells intervention after elevation of intraocular pressure in the rat, Acta Ophthalmol. 90 (2012) e560–e567.

[13] M. Shafaati, N. Mast, O. Beck, R. Nayef, G.Y. Heo, L. Bjorkhem-Bergman, D. Lutjohann, I. Bjorkhem, I.A. Pikuleva, The antifungal drug voriconazole is an efficient inhibitor of brain cholesterol 24S-hydroxylase in vitro and in vivo, J. Lipid Res. 51 (2010) 318–323.

[14] M. Simitsopoulou, E. Roilides, C. Likartsis, J. Ioannidis, A. Orfanou, F. Paliogianni, T.J. Walsh, Expression of immunomodulatory genes in human monocytes induced by voriconazole in the presence of *Aspergillus fumigatus*, Antimicrob. Agents Chemother. 51 (2007) 1048–1054.

[15] H. Gao, M.E. Pennesi, K. Shah, X. Qiao, S.M. Hariprasad, W.F. Mieler, S.M. Wu, E.R. Holz, Intravitreal voriconazole: an electroretinographic and histopathologic study, Arch. Ophthalmol. 122 (2004) 1687–1692.

[16] J. Harrison, R. Glickman, C. Ballentine, Y. Trigo, M. Pena, P. Kurian, L. Najvar, N. Kumar, A. Patel, W. Sponsel, J. Graybill, W. Lloyd, M. Miller, G. Paris, F. Trujillo, A. Miller, R. Melendez, Retinal function assessed by ERG before and after induction of ocular *Aspergillosis* and treatment by the anti-fungal, Micafungin, in Rabbits, Doc. Ophthalmol. 110 (2005) 37–55.

[17] J. Kinoshita, N. Iwata, M. Ohba, T. Kimotsuki, M. Yasuda, Mechanism of voriconazole-induced transient visual disturbance: reversible dysfunction of retinal ON-bipolar cells in monkeys, Invest. Ophthalmol. Vis. Sci. 52 (2011) 5058–5063.

[18] C. Schnebelen, B. Pasquis, M. Salinas-Navarro, C. Joffre, C.P. Creuzot-Garcher, M. Vidal-Sanz, A.M. Bron, L. Bretillon, N. Acar, A dietary combination of omega-3 and omega-6 polyunsaturated fatty acids is more efficient than single supplementations in the prevention of retinal damage induced by elevation of intraocular pressure in rats, Graefes Arch. Clin. Exp. Ophthalmol. 247 (2009) 1191–1203.

[19] G.B. Jaissle, C.A. May, J. Reinhard, K. Kohler, S. Fauser, E. Lutjen-Drecoll, E. Zrenner, M.W. Seeliger, Evaluation of the rhodopsin knockout mouse as a model of pure cone function, Invest. Ophthalmol. Vis. Sci. 42 (2001) 506–513.

[20] H.A. Hancock, T.W. Kraft, Oscillatory potential analysis and ERGs of normal and diabetic rats, Invest. Ophthalmol. Vis. Sci. 45 (2004) 1002–1008.

[21] L. Alarcon-Martinez, M. Aviles-Trigueros, C. Galindo-Romero, J. Valiente-Soriano, M. Agudo-Barriuso, L. Villa Pde, M.P. Villegas-Perez, M. Vidal-Sanz, ERG changes in albino and pigmented mice after optic nerve transection, Vision Res. 50 (2010) 2176–2187.

[22] J. Folch, M. Lees, G.H. Sloane Stanley, A simple method for the isolation and purification of total lipides from animal tissues, J. Biol. Chem. 226 (1957) 497–509.

[23] N. Mast, C. Charvet, I.A. Pikuleva, C.D. Stout, Structural basis of drug binding to CYP46A1, an enzyme that controls cholesterol turnover in the brain, J. Biol. Chem. 285 (2010) 31783–31795.

[24] N. Cuenca, I. Pinilla, L. Fernandez-Sanchez, M. Salinas-Navarro, L. Alarcon-Martinez, M. Aviles-Trigueros, P. de la Villa, J. Miralles de Imperial, M.P. Villegas-Perez, M. Vidal-Sanz, Changes in the inner and outer retinal layers after acute increase of the intraocular pressure in adult albino Swiss mice, Exp. Eye Res. 91 (2010) 273–285.

[25] L. Alarcon-Martinez, P. de la Villa, M. Aviles-Trigueros, R. Blanco, M.P. Villegas-Perez, M. Vidal-Sanz, Short and long term axotomy-induced ERG changes in albino and pigmented rats, Mol. Vis. 15 (2009) 2373–2383.

[26] N. Acar, B. Bonhomme, C. Joffre, A.M. Bron, C. Creuzot-Garcher, L. Bretillon, M. Doly, J.M. Chardigny, The retina is more susceptible than the brain and the liver to the incorporation of trans isomers of DHA in rats consuming trans isomers of alpha-linolenic acid, Reprod. Nutr. Dev. 46 (2006) 515–525.

[27] T. Nakazawa, T. Hisatomi, C. Nakazawa, K. Noda, K. Maruyama, H. She, A. Matsubara, S. Miyahara, S. Nakao, Y. Yin, L. Benowitz, A. Hafezi-Moghadam, J.W. Miller, Monocyte chemoattractant protein 1 mediates retinal detachment-induced photoreceptor apoptosis, Proc. Natl. Acad. Sci. USA 104 (2007) 2425–2430.

[28] M. Rutar, R. Natoli, K. Valter, J.M. Provis, Early focal expression of the chemokine Ccl2 by muller cells during exposure to damage-inducing bright continuous light, Invest. Ophthalmol. Vis. Sci. 52 (2011) 2379–2388.

[29] J.K. Krady, A. Basu, C.M. Allen, Y. Xu, K.F. LaNoue, T.W. Gardner, S.W. Levison, Minocycline reduces proinflammatory cytokine expression, microglial

activation, and caspase-3 activation in a rodent model of diabetic retinopathy, Diabetes 54 (2005) 1559–1565.
[30] H. Levkovitch-Verbin, M. Kalev-Landoy, Z. Habot-Wilner, S. Melamed, Minocycline delays death of retinal ganglion cells in experimental glaucoma and after optic nerve transection, Arch. Ophthalmol. 124 (2006) 520–526.
[31] C. Zhang, B. Lei, T.T. Lam, F. Yang, D. Sinha, M.O. Tso, Neuroprotection of photoreceptors by minocycline in light-induced retinal degeneration, Invest. Ophthalmol. Vis. Sci. 45 (2004) 2753–2759.
[32] A. Bosco, D.M. Inman, M.R. Steele, G. Wu, I. Soto, N. Marsh-Armstrong, W.C. Hubbard, D.J. Calkins, P.J. Horner, M.L. Vetter, Reduced retina microglial activation and improved optic nerve integrity with minocycline treatment in the DBA/2J mouse model of glaucoma, Invest. Ophthalmol. Vis. Sci. 49 (2008) 1437–1446.